Study of mitotic chromatin shows involvement of histone modifications in bookmarking and reveals nucleosome deposition patterns

Elisheva Javasky[1,*], Inbal Shamir[1,*], Shashi Gandhi[1], Shawn Egri[2], Oded Sandler[1], Noam Kaplan[3], Jacob D. Jaffe[2], Alon Goren[4,#], Itamar Simon[1,#]

1 Department of Microbiology and Molecular Genetics, Institute of Medical Research Israel-Canada, Faculty of Medicine, The Hebrew University, Jerusalem 91120, Israel

2 The Broad Institute of Harvard and MIT, Cambridge, MA 02142 USA

3 Department of Physiology, Biophysics & Systems Biology, Rappaport Faculty of Medicine, Technion Israel Institute of Technology, Haifa, Israel

4 Department of Medicine, University of California, San Diego, La Jolla California, USA

* These authors contributed equally to this study

Correspondence to: Itamar Simon itamarsi@ekmd.huji.ac.il and Alon Goren agoren@ucsd.edu

Abstract

Mitosis encompasses key molecular changes including chromatin condensation, nuclear envelope breakdown and reduced transcription levels. Immediately after mitosis, the interphase chromatin structure is reestablished and transcription resumes. The reestablishment of the interphase chromatin requires 'bookmarking', *i.e.*, the retention of at least partial information during mitosis. Yet, while recent studies demonstrate that chromatin accessibility is generally preserved during mitosis and is only locally modulated, the exact details of the bookmarking process and its components are still unclear. To gain a deeper understanding of the mitotic bookmarking process, we merged proteomics, immunofluorescence, and ChIP-seq approaches to study the mitotic and interphase organization in human cells. We focused on key histone modifications, and employed the HeLa-S3 cells as a model system. Generally, we observed a global concordance between the genomic organization of histone modifications in interphase and mitosis, yet the abundance of the two types of modifications we investigated was different. Whereas histone methylation patterns remain highly similar, histone acetylation patterns show a general reduction while maintaining their genomic organization. In line with a recent study demonstrating that minimal transcription is retained during mitosis, we show that RNA polymerase II does not fully disassociate from the genome, but rather maintains its genomic localization at reduced levels. Next, we followed up on previous studies demonstrating that nucleosome depleted regions (NDRs) become occupied by a nucleosome during mitosis. Surprisingly, we observed that the nucleosome introduced into the NDR during mitosis encompasses a distinctive set of histone modifications, differentiating it from the surrounding nucleosomes. We show that the nucleosomes in the vicinity of the NDR appear to both shift into the NDR during mitosis and undergo deacetylation. HDAC inhibition by the small molecule TSA reverts the deacetylation pattern of the shifted nucleosome. Taken together, our results demonstrate that the epigenomic landscape can serve as a major component of the mitotic bookmarking process, and provide evidence for a mitotic deposition and deacetylation of the nucleosomes surrounding the NDR.

Introduction

The cell cycle is a dynamic orchestrated process that involves major changes to the chromatin structure (Raynaud et al. 2014) and the expression of hundreds of genes (Spellman et al. 1998; Cho et al. 2001; Whitfield et al. 2002; Bar-Joseph et al. 2008). During the cell cycle, DNA is replicated along S-phase and then condensed in mitosis prior to cell division.

During mitosis the cell undergoes profound changes. The nuclear envelope breaks apart and the chromosomes change their shape into distinguishable thick structures. Multiple studies have examined the structure of mitotic chromosomes using microscopy (Vagnarelli 2013), but they lack fine-detail information on individual loci. Recently, genome-wide long-range interactions within mitotic chromosomes were investigated by HiC and 4C (Naumova et al. 2013; Dileep et al. 2015; Stevens et al. 2017). These studies demonstrate the disappearance of consistent high order chromatin structure in mitosis, including both genome compartments and topological associated domains (TADs). Nevertheless, the unique features of mitotic chromatin at a finer genomic resolution remain unexplored. In addition to chromosome reshaping, mitotic chromosomes are characterized by the disassociation of numerous proteins including RNA polymerase II and many gene-specific and general transcription factors (Martinez-Balbas et al. 1995; Parsons and Spencer 1997; Kadauke and Blobel 2013). The disassociation of these transcription machinery components leads to a dramatic decrease in transcription (King and Barnhisel 1967; Gottesfeld and Forbes 1997; Liang et al. 2015; Palozola et al. 2017), with the exception of several genes, which maintain their transcription during mitosis (Liang et al. 2015; Li et al. 2017; Palozola et al. 2017)

Immediately after mitosis, the chromatin structure is gradually reestablished – the chromosomes decondense throughout G1 (Belmont and Bruce 1994), the interphase TAD structures are re-formed within four hours after cytokinesis (Dileep et al. 2015), and transcription is reinitiated at the beginning of G1 (Prescott and Bender 1962; Gottesfeld and Forbes 1997; Prasanth et al. 2003). This complex orchestration of TAD re-formation and controlled transcription re-initiation necessitates precise epigenomic markings, which therefore must be preserved during mitosis, despite the radical changes to the chromatin. How is this epigenomic information stored during mitosis? The current view is that partial information is retained on mitotic chromosomes to serve as bookmarks for the reestablishment of the chromatin structure. In line with that, even in their condensed state, mitotic chromosomes remain accessible as is evident by both biophysical measurements (Chen et al. 2005; Caravaca et al. 2013) and DNase I sensitivity assays (Gazit et al.

1982; Kadauke et al. 2012). Furthermore, genomic chromatin accessibility maps by DNaseI sensitivity and ATAC-seq comparing mitotic and interphase cells revealed that the accessibility is generally preserved and is only locally modulated during mitosis (Hsiung et al. 2015; Teves et al. 2016). Yet, it remains unclear what serves as the bookmarks for the restoration of the global chromatin structure following the changes occurring during mitosis.

Much effort has been devoted to identifying components of the transcription machinery that may serve as cell cycle bookmarks. These studies focused mainly on general and specific transcription factors that are retained at a subset of their locations during mitosis (reviewed in (Kadauke and Blobel 2013; Zaidi et al. 2014)). Additionally, preliminary evidence suggests that histone tail modifications themselves participate in carrying out the task of bookmarking. It has been reported that retaining H4K5ac levels during mitosis is crucial for the bookmarking of a reporter gene (Zhao et al. 2011). Furthermore, the global levels of several histone modifications were shown to be preserved during mitosis (reviewed in (Wang and Higgins 2013)). However, the mitotic histone modification levels were mostly assessed globally (*e.g.,* by methods such as western blots, mass spectrometry, or immuno-staining), and therefore lacked spatial genomic information, with few exceptions where ChIP experiments demonstrated a mitotic preservation of histone acetylations at the promoters of several transcribed genes (Kouskouti and Talianidis 2005; Valls et al. 2005). An initial clue regarding the genome-wide organization of histone modifications was achieved by employing ChIP-seq to map H3K4me3, H3K27ac, and H2A.Z in interphase and mitotic cells. Interestingly, the genome-wide maps of H3K4me3 and H2A.Z revealed that the general genomic localization of these marks is conserved upon mitosis entry (Kelly et al. 2010; Liang et al. 2015). Conversely, most H3K27ac genome-wide studies describe a degree of locus specificity in the maintenance of H3K27ac during mitosis (Hsiung et al. 2016; Li et al. 2017; Liu et al. 2017a; Liu et al. 2017b).

Intriguingly, while the genomic localization of H3K4me3 and H2A.Z appears to be highly concordant between mitosis and interphase, the patterns of these histone marks were shown to dramatically differ between mitosis and interphase in specific genomic areas termed NDRs (nucleosome depleted regions) (Kelly et al. 2010; Liang et al. 2015). NDRs are loci highly depleted of nucleosomes, and hence differ from the mostly uniform distribution of nucleosomes across the genome (Lee et al. 2004). NDRs are mainly located within promoters and enhancers, and thus are enriched with RNA polymerase and transcription factor binding sites (Henikoff 2008; Tsompana and Buck 2014). Promoter associated NDRs were shown to disappear during mitosis, and contain a nucleosome harboring H3K4me3 (Liang et al. 2015) and H2A.Z (Kelly et

al. 2010). However, the histone composition of the nucleosomes that occupy these NDRs, as well as the NDR occupation mechanism remains unclear.

To better understand the role of mitotic histone modifications and nucleosome depositioning in bookmarking, we investigated the global dynamics and genomic organization of histone modifications in mitosis and in interphase. Using HeLa-S3 cells as a model system, our study incorporated a synchronization approach that enables the collection of relatively pure preparations of mitotic cells; proteomics analysis focused on quantitative evaluation of the global levels of histone modifications; and systematic genome localization mapping of RNA polymerase II (RNA PolII) and six key histone modifications (H3K4me1, H3K4Me3, H3K9ac, H3K27ac, H3K27me3, and H3K36me3).

Our results demonstrate that the histone modification levels and patterns are generally concordant between interphase and mitosis, with one main exception: while histone methylations remain highly similar, histone acetylations show a general reduction in mitosis. Additionally, in line with a recent study demonstrating that minimal transcription is retained during mitosis (Palozola et al. 2017), we provide evidence showing that RNA PolII does not fully disassociate from the genome, but rather maintains its genomic localization at reduced levels. Finally, analysis of NDRs associated with transcription start sites (TSSs), putative enhancers and putative insulators revealed that the nucleosome occupying the NDR during mitosis is distinguishable from the surrounding nucleosomes, and characterized by a distinctive set of histone modifications. We propose that the nucleosome in the vicinity of the interphase NDR (*e.g.*, the +1 nucleosome for TSSs) shifts to the NDR during mitosis and undergoes deacetylation by HDACs. Small molecule inhibition of HDACs reverts the deacetylation pattern of the shifted nucleosome, lending support to our model. Taken together, our results demonstrate that the epigenomic landscape can serve as a major component of the mitotic bookmarking process. Additionally, we provide evidence for a mitotic deposition and deacetylation of the nucleosomes surrounding the NDR.

Results

Efficient metaphase synchronization of HeLa-S3cells using a kinesin 5 inhibitor (STC)

Mitotic cells comprise about 2% of a non-synchronized interphase population. Thus, determining the chromatin landscape by proteomics and ChIP-seq of this cell cycle phase requires the generation of relatively pure preparations of mitotic cells. The kinesin 5 inhibitor STC (Skoufias et al. 2006) inhibits both separation of the duplicated centrosomes and bipolar spindle formation,

resulting in cells arrested in metaphase with monoastral spindles (**Figure 1A)**. Following treatment of HeLa-S3 cells with STC we were able to achieve very tight synchronization with an average of approximately 90% (SE = 1.6%; n=8) of cells in the metaphase stage of mitosis (**Figure 1B**). STC provides tight synchronization at the metaphase stage whereas other synchronization approaches such as nocodazole, arrest cells at the prophase/prometaphase stage (Matsui et al. 2012). Hence, we preferred the STC based approach to enable the study of mitotic chromatin. For simplicity, we refer below to the unsynchronized population as "interphase" cells and to the synchronized one as "mitosis".

RNApol-II binding is maintained during mitosis at low levels

In accordance with previous studies (Parsons and Spencer 1997), we observed a dramatic reduction in RNA PolII occupancy in the mitotic samples, reflecting a higher percentage of nonspecific binding (**Figure 1C-D**). Nevertheless, in both interphase and mitotic samples, PolII binding was almost exclusively at promoters (**Figure S1**). Recent findings suggest that the cell's transcription pattern is largely retained at a low level throughout mitosis (Palozola et al. 2017). In light of these observations, we evaluated whether the low occupancy of PolII in mitosis reflects real mitotic binding or is a consequence of the up to 10% contamination of interphase cells in the mitotic samples (**Figure 1 B**). To this end, we simulated the interphase contamination effect by mixing 10% of the interphase reads together with 90% of the reads in a control experiment. In accordance with the Palozola *et al*. results, we found a clear difference between the simulation experiment and the real mitotic ChIP-seq data (**Figure 1 C-D**). This suggests that PolII is retained on most of the promoters at low levels.

Identification of global changes in histone modifications via mass-spectrometry based proteomic analysis

To gain insight into the global changes in histone modifications during mitosis, we employed a quantitative mass-spectrometry (MS) based approach (Jaffe et al. 2013). By implementing synthetic peptide standards, this MS approach provides high reproducibility and is ideal for comparing the levels of histone modifications between mitosis and interphase. Using this method, we profiled the patterns of histone modifications in three biological replicates of mitotic and interphase samples. In line with previous observations (Hendzel et al. 1997; Van Hooser et al. 1998; Johansen and Johansen 2006), the H3S10ph modification was highly enriched in the mitotic samples compared to interphase (~17 folds; Pval<10^{-3}; two sided t-test; **Figure 2**), lending

additional support to our synchronization approach. We further estimated the absolute percentage occupancy of individual histone marks by comparing mass spectral intensity vs. known concentrations of internal standards and summarizing the results. While the global levels of histone methylations were mostly similar between mitosis and interphase, histone acetylations were reduced in mitotic samples (~3-6 fold reduction; Pval <0.015; two sided t-test; **Figure 2).**

We confirmed the distinction between histone methylation and acetylation by performing quantitative immunofluorescence and measuring the mitotic and interphase levels of H3K9ac and H3K4me3. While the levels of H3K4me3 were almost identical in mitosis and interphase as measured by immunofluorescence, H3K9ac levels were 2.7 folds lower in mitosis ($P< 10^{-23}$; t-test; **Figure S3**). Together, these observations reveal a key distinction between the protein level dynamics of histone acetylation versus methylation in the transition from interphase to mitosis. However, these results do not show how this difference is reflected spatially in the genomic organization of these histone modifications.

Analysis of the epigenomic landscape reveals high concordance between mitotic and interphase localization of histone marks

To follow up on the observation we got from the proteomics analysis and compare the genomic organization of histone marks between mitosis and interphase, we performed ChIP-seq focusing on key histone modifications. We chose six major histone modifications that together capture main chromatin features including active promoters (H3K4me3, H3K9ac, and H3K27ac), putative enhancers (H3K4me1 and H3K27ac that is also associated with active promoters), gene bodies (H3K36me3), and repressed regions (H3K27me3) (Zhou et al. 2011) (**Figure 3**). Surprisingly, we found no major changes between the overall epigenomic landscapes of the mitotic and interphase samples, in two biological replicates (**Figure 3A** and **Figure S4**). While this observation was true for all histone modifications examined, there is a clear distinction between methylation marks, which seem to remain intact, and acetylation marks, which show a universal and uniform signal reduction in mitosis (**Figure 3B**). This is in line with our proteomics and immunofluorescence observations regarding the global levels of these modifications in these cell cycle phases.

To quantify the genomic changes in the modification levels between mitosis and interphase, we used the ENCODE mappings of chromatin environments derived from the combined ChromHMM annotations (Ernst and Kellis 2012). We compared the distributions of the histone modifications between interphase and mitosis, and found that the distribution of the methylation

signal in interphase and mitosis was almost identical. Conversely, the genomic distribution of the H3K27 and H3K9 acetylations differed slightly between these cell cycle phases and both modifications presented an increase in the signal over enhancer regions (5% and 2%; respectively), and concurrent reduction in the promoter signal (6% and 3%; respectively) in mitosis (**Figure 3C**).

The nucleosome-depleted regions (NDRs) become occupied during mitosis by a nucleosome distinguishable from its neighbors

Previous reports demonstrated that nucleosome depleted regions (NDRs) associated with the transcription start site (TSS) of promoters are lost during mitosis, and the gap is occupied by a nucleosome containing H3K4me3 and H2A.Z (Kelly et al. 2010; Liang et al. 2015). To better understand this mitotic change in the chromatin structure, we leveraged the variety of histone modifications we mapped in mitosis and interphase to study the histone modifications of the nucleosome that occupies the NDR during mitosis. The range of marks enabled the investigation of NDRs associated with promoters, putative enhancers, and insulators for the first time.

First, we focused on H3K4me3, which was previously shown to occupy promoter NDRs during mitosis (Liang et al. 2015). In line with Liang *et al*.'s report, the datasets we generated were mostly devoid of the promoter NDR structure in mitosis (**Figure 4A**), even though our samples were synchronized using a different approach (STC vs. nocodazole). Additionally, extension of this analysis to include putative enhancers and insulators, revealed that in mitosis, a nucleosome containing methylated histones also occupies NDRs associated with these regulatory regions (**Figures 4A, S5 - S7**).

Surprisingly, when we analyzed the organization of the histone acetylations H3K9ac and H3K27ac over NDRs, the binding structure was mostly preserved during mitosis as opposed to the pattern observed for the histone methylations, suggesting that the nucleosome occupying the NDR is deacetylated (**Figures 4B and S5-S7**). To corroborate our observation, we analyzed data from G1E murine erythroblast cells (Hsiung et al. 2016). Consistently, in G1E murine cells the nucleosome occupying the NDR is mostly deacetylated (**Figure S8**), indicating that this phenomenon is conserved between species and cell types. Altogether, these data demonstrate that the nucleosomes occupying NDRs during mitosis are methylated but not acetylated, hence distinguishable from the neighboring nucleosomes that are dually marked by both methylation and acetylation.

Classification of the NDRs according to nucleosome modifications during mitosis

To further characterize the nucleosomes that occupy the NDR during mitosis, we looked at the coverage profiles of genes marked with H3K4me3, H3K9ac, and H3K27ac at their TSSs, and sorted the profiles by occupancy of mitotic H3K9ac at the TSS. The sorted profiles revealed four gene groups based on the combination of modifications occupying the NDR (**Figures 5A-B, and S9**). The groups were classified as follows: *Group 1*: retention of the NDR during mitosis. *Group 2*: loss of the NDR during mitosis due to the entry of a nucleosome with solely methylated histones. *Group 3*: loss of the NDR during mitosis due to entry of a nucleosome with both methylated and acetylated histones. *Group 4:* absence of an NDR in both interphase and mitosis. We disregarded *Group 4* from further analyses since it already lacked an NDR in interphase. Of the promoters analyzed, we found that approximately 22% belong to *Group 1*, 61% to *Group 2*, and 9% to *Group 3*.

To characterize *Groups 1-3*, we first compared the percentage of GC in each group and found that *Group 1* has a higher GC content than *Groups 2* and *3* (approximately 70% vs 62% and 60% in *Groups 2* and *3*, respectively; **Figure 5C**). Thus, the GC content appears to distinguish between regions that retain the NDR during mitosis and regions that lose it, regardless of the modifications of the histones on the nucleosomes. As GC content may be associated with the binding of specific transcription factors (TFs), we next employed DREME, a discriminative motif discovery tool (Bailey 2011), to identify motifs enriched in *Group 1* relative to the other groups. Indeed, along with the high GC content observed in *Group 1*, many of the motifs were enriched for GC (**Figure S10).**

To further investigate the characteristics of these three groups, we studied the binding patterns of TFs mapped by ENCODE in HeLa-S3 cells. Similar to the GC content distinction, most of the TFs (*e.g.*, HCF1, NFYB, BRCA1 and MXI1; **Figures 5D and S11**) demonstrated a binding pattern that differed between *Group 1* and the two other groups (*2* and *3*), whereas only a limited number of factors (*e.g.,* E2F1 and USF2; **Figures 5D and S11**) show distinct binding patterns for each of the groups. This observation, together with the GC content results, suggest that there is an initial division between genes that have a nucleosome in the NDR during mitosis versus genes that do not.

Next, to better understand what distinguishes *Group 2* from *Group 3*, we evaluated the association of HDAC binding to each of these groups. Analysis of our and public HDAC ChIP-

seq data (Wang et al. 2009; Ram et al. 2011) revealed a statistically significant difference between these groups: 43% of the TSSs in *Group 2*, whose nucleosomes are deacetylated, overlapped with an HDAC peak, while only 35% of the TSSs in *Group 3*, whose nucleosomes are acetylated, were occupied by an HDAC (p-value ~ 0.001; Chi squared test). Thus, it appears that the presence of HDAC may contribute to the observed difference in the acetylation patterns.

Mitosis associated nucleosome deposition into the NDR

Nucleosome occupancy at NDRs during mitosis was previously explained as a consequence of the penetration of the +1 nucleosome into the NDR (Kelly et al. 2010). However, the absence of acetylation of this nucleosome challenges this model. We envisioned two possible models for the integration of the nucleosome in the NDR during mitosis. The *first model* being the incorporation into the NDR of a new nucleosome whose histones are methylated but not acetylated. The *second model* proposes, as postulated previously, that the surrounding nucleosomes shift into the NDR in mitosis, and the histones are actively deacetylated by HDACs (histone deacetylases).

To discriminate between the two models, we first evaluated the dynamics of H3K4me3 in interphase and mitotic samples. H3K4me3 was shown by both a previous study and our analysis to occupy the NDR during mitosis. To evaluate the nucleosome movements from our data, we measured the difference in the signal in mitosis compared to the coverage in interphase for the promoter NDRs in H3K4me3 data (Delta plots; see methods). We observed that the increase in nucleosome occupancy at the TSS is followed by a decrease in nucleosome occupancy in the downstream regions, suggesting a shift of the +1 nucleosome into the NDR. This observation is in line with Kelly *et al*.'s findings (Kelly et al. 2010). Further, we identified similar patterns, where the surrounding nucleosomes enter the NDR during mitosis, also at enhancers and insulators (**Figure 6A**).

Next, to further validate the second model, we treated interphase and mitotic cells with the global HDAC inhibitor TSA. Perturbation of HDAC activity eliminates the general mitotic hypoacetylation, and ChIP-seq performed on purebred samples demonstrates a highly similar H3K9ac localization patterns in interphase and mitosis (**Figure 6B**). Additionally, inhibition of HDAC activity altered the histone acetylation pattern we observed previously at the NDRs, and in TSA treated mitotic cells the nucleosomes occupying the NDRs have acetylated histones (**Figure 6C**). Delta plots demonstrated that the increase in the levels of acetylated histone in the NDR is accompanied by a decrease in the signal at the surrounding regions. This further supports the

notion that this nucleosome shifts into the NDR from a surrounding position (**Figure 6D**). A similar observation was seen in enhancer and insulator regions (**Figure S14**). Finally, H3K4me3 patterns were not affected by TSA treatment, thereby negating the possibility of a global effect (**Figure S15**).

Discussion

In this study, we aimed to gain a better understanding of the mitotic bookmarking process and the organization of chromatin during this phase. We designed an interdisciplinary approach that merges proteomics, immunofluorescence, automated ChIP-seq, and computational analysis to allow robust identification of changes between interphase and mitosis. Incorporating biological replicates for all measurements, we obtained quantitative details regarding the global amounts of modified histones in each cell cycle phase by employing MS and immunofluorescence, and generated genome-wide chromatin maps for RNA PolII and six key histone modifications. These epigenomic landscapes provide insight into the spatial chromatin organization during interphase and mitosis. To the best of our knowledge, we are the first to conduct this kind of systematic molecular survey, combining global (proteomics and immunofluorescence) and spatial (epigenomics) measurements in interphase and mitosis.

Analyzing the proteomic and epigenomic datasets provided several major insights. We observed that although mitotic chromatin is highly condensed, global levels of histone methylations are mostly maintained. Nevertheless, histone acetylation abundance was reduced in mitotic samples both at the global protein level (via proteomics and immunofluorescence), and at the level of association with DNA (via ChIP-seq). Yet, the change in acetylation levels between mitosis and interphase was moderate (about 2-6 fold) compared, for instance, to the variation observed in H3S10ph levels (about 17 fold) between these two phases (**Figure 2**). Furthermore, comparison of the genomic localization between interphase and mitotic samples demonstrated that the organization of these modifications was tightly maintained. Altogether, apart from the patterns we observed in NDRs and discuss below, we did not identify local differences in the organization of the histone modification patterns between mitosis and interphase, suggesting that the genome undergoes global, uniform changes during mitosis.

The observation that histone modification patterns are concordant between interphase and mitosis lends support to the hypothesis that the preserved genomic organization of these marks plays a bookmarking role. This model is an important addition to our understanding of the epigenomic memory during the cell cycle. For many years mitotic chromosomes were considered to be

transcriptionally silenced (Taylor 1960; Prescott and Bender 1962; Parsons and Spencer 1997), devoid of most transcription factors (Martinez-Balbas et al. 1995; Gottesfeld and Forbes 1997; Prasanth et al. 2003), and condensed (Antonin and Neumann 2016). Thus, it was unclear how epigenomic information is transmitted throughout the cell cycle. Initial studies have demonstrated that bookmarking is carried out by a limited number of transcription factors that are retained on the chromosomes during mitosis to enable the reestablishment of the transcriptional program in G1 (Kadauke et al. 2012; Kadauke and Blobel 2013).

In contrast, our study suggests that the overall epigenomic structure in interphase is vastly maintained during mitosis, thus quashing the need for bookmarking factors altogether. This observation is in line with several recent studies, which indicate various levels of similarity between, mitotic and interphase chromatin structure. First, it was shown both in drosophila and mice that a large portion of the transcription machinery, including many transcription factors and chromatin regulators, remain on the chromosomes during mitosis (Black et al. 2016; Teves et al. 2016; Liu et al. 2017b). Second, a genome-wide DNase-seq experiment revealed that genome accessibility is widely preserved and only locally modulated during mitosis (Hsiung et al. 2015). Finally, a recent study utilized 5EU labeling to demonstrate that many genes exhibit transcription during mitosis (Palozola et al. 2017). Taken together, these and our observations suggest that in spite of their condensation, mitotic chromosomes retain a base level of their original chromatin structure and are partially involved in active transcription, thus alleviating the requirement for additional bookmarking.

Recently, several studies employed ChIP-seq to assess histone modification levels during mitosis. There are however, conflicting observations regarding the direction and uniformity of the changes in mitotic H3K27ac. While we observed a uniform decrease in H3K27ac levels in mitosis relative to interphase (**Figures 2 and 3B**), a recent study in breast cancer MCF-7 cells saw a uniform increase in the levels of this modification in mitotic cells (Liu et al. 2017a). Other studies demonstrated that the change in H3K27ac levels in mitosis is heterogeneous (Hsiung et al. 2016; Liu et al. 2017b). We cannot rule out the possibility that these variations are a consequence of technical differences (*e.g.*, synchronization techniques) between the studies. However, the variations may also reflect a biological distinction between fully differentiated cells and cells that carry the potential for further differentiation. In line with this notion, mitosis constitutes a window of opportunity for altering cellular fates via mitotic chromatin reprogramming (Halley-Stott et al. 2014). Thus, H3K27ac, a modification linked to cell fate decisions (Long et al. 2016), may exhibit a heterogeneous change in profile in cells possessing the potency to differentiate

(ESC and G1E erythroblasts), and a uniformly changing profile in fully differentiated cells (HeLa-S3 and MCF-7).

While we observed retention of the epigenomic organization during mitosis both for histone methylations and acetylations, there was a uniform genome-wide deacetylation of histone H3K9 and H3K27. Global deacetylation of histones during mitosis has been observed before, but its precise role in mitosis is not fully understood. An early study revealed that blocking deacetylation by HDAC inhibition shortly before mitosis in human primary fibroblasts causes severe mitotic defects (Cimini et al. 2003). It has also been shown that independent of its role in transcription regulation, histone deacetylation during mitosis plays a structural role in mediating Aurora B-dependent phosphorylation of mitotic chromosomes, which is important for their condensation (Li et al. 2006). On the other hand, other studies have suggested a transcription dependent mechanism (Noh et al. 2009), which would presumably be locus specific. Thus, our results, which show a uniform genome-wide deacetylation of H3K9 and H3K27, strongly support the structural role of the deacetylation over a transcription dependent mechanism.

Previous studies demonstrated that during mitosis there is a shift of the +1 nucleosome into the NDR that is associated with transcription start sites (Kelly et al. 2010; Liang et al. 2015). Yet, as these studies focused either on H2A.Z (Kelly et al. 2010) or H3K4me3 (Liang et al. 2015), there was no data regarding other components of the nucleosome that occupies the NDR in mitosis. Furthermore, it was unclear whether this phenomenon is restricted to NDRs associated with promoters, or if it is global and can also occur in regions associated with enhancers or insulators.

Leveraging the comprehensive paired datasets we generated for interphase and mitosis, we were able to expand upon these initial observations and study a comprehensive set of histone modifications as well as the NDRs associated with enhancers and insulators. We observed that while our H3K4me3 data exhibited very similar patterns as seen by the Shilatifard group (Liang et al. 2015), the nucleosome occupying the NDR in mitosis was devoid of histone acetylations H3K9ac and H3K27ac. This is a very intriguing observation, as it implies that the nucleosome entering the NDR during mitosis differs from its neighboring nucleosomes, which comprise H3K4me3, H3K9ac, and H3K27ac. By analyzing public H3K27ac data from murine erythroblast cells, we showed that this NDR structure is also found in mouse cells, suggesting that the acetylation pattern we observed is evolutionarily conserved.

The role of the mitotic movement of the nucleosome into the NDR is not clear. It may be a mere

consequence of the eviction of RNA polymerase and other factors that frees up the DNA at the NDR to become occupied by adjacent nucleosomes. However, the specific deacetylation that takes place precisely on the histones that move into the NDR likely requires a designated mechanism, evidence that this process is biologically important. Recently, it was postulated that nucleosomes play a role in potentiating transcription (Nagai et al. 2017). Thus, it is possible that the penetration of the nucleosomes into the NDR during mitosis is involved in restoring transcription immediately after mitosis.

Following our observation that the nucleosome penetrating the NDR during mitosis has a distinctive composition of modifications, we have shown that the deacetylation of this nucleosome is HDAC dependent (**Figure 6**). However, the exact mechanism localizing the deacetylation specifically to this nucleosome is still unclear. We and others have previously shown that HDACs bind tightly at the TSS (Wang et al. 2009; Ram et al. 2011). This suggests that HDAC positioning may play a role in the specific deacetylation of the shifting nucleosome at this region. Alternatively, the shifting nucleosome may be more dynamic than the others, thus during its partial disassociation from the DNA it can become deacetylated. Indeed, it has been shown that histones associated with promoter and regulatory regions are less stable than histones localized at other genomic loci (Jin and Felsenfeld 2007).

The biological role of the specific deacetylation of the nucleosome that shifts into the NDR is also not clear. An appealing hypothesis is that this deacetylation serves to bookmark the region as an NDR in interphase, and enables the removal of the penetrating nucleosome immediately after mitosis. In line with this hypothesis, it has been shown that some chromatin remodeling complexes are influenced by histone modifications (Swygert and Peterson 2014), supporting the possibility that the deacetylation facilitates the removal of this nucleosome by recruiting specific remodeling complexes immediately after mitosis.

Not all NDRs undergo the same mitosis-associated changes. We found that in most cases the penetrating nucleosome is indeed deacetylated, however there is a large group of promoters in which no nucleosome penetrates the NDR during mitosis. Interestingly, these promoters are already distinguishable from the others during interphase in several ways: (***i***) these regions have a higher GC content; (***ii***) the binding of many TFs is less localized to the TSS of these promoters (**Figure 5**); and (***iii***) the NDR seems to be wider (see for example the H3K4me3 plot in **Figure S12**). Taken together, these findings suggest that basic differences in the promoter architecture reflect the mechanism that preserves the NDR during interphase. Only some of the mechanisms

associated with these different promoter architectures are active during mitosis, and this may explain the differential loss of some NDRs. Thus for example, sequence based mechanisms should be preserved during mitosis whereas cases in which the interphase NDR is kept due to transcription factors associated with the DNA (Struhl and Segal 2013), may be lost during mitosis. Further work is needed to understand these mechanisms and their importance in mitotic function.

Overall, together with several recent studies, our work provides an important cornerstone necessary for shifting the paradigm that has lingered for many years. We can reason that while structurally the chromatin goes through major changes during mitosis, molecular characteristics such as the organization of histone modifications are maintained, even if the levels are reduced. This provides a simpler explanation for the restoration of chromatin structure following mitosis.

Material and methods

Cell Culture and synchronization

HeLa-S3 cells were grown in Spinner flasks in Dulbecco's modified Eagle's medium (DMEM) supplemented with 10% Fetal Bovine Serum (FBS), Penicillin-Streptomycin, L-Glutamine, Sodium Pyruvate and 0.1% Pluronic F-68. Cells were incubated at 37^0C and 5% CO_2. Cells were pre-synchronized in G1/S by addition of 2mM thymidine for 16 hrs, washed with PBS, released for 3 hrs in fresh medium and arrested with S-Trityl-L-cysteine (STC) (164739, Sigma) for 12 hrs. HDAC blocking was done with 150nM Trichostatin A (TSA, T1952, SIGMA) which was added either to unsynchronized culture or 3 hours after adding the STC for 9 hours.

Immunofluorescence and Microscopy

Cells were fixed with either 70% ethanol or 4% paraformaldehyde, blocked with 5% BSA, and stained either with mouse anti LaminA (1:1000; L1293, Sigma) followed by donkey anti-mouse DyLight® 550 (1:400; ab98795, Abcam), or by rabbit anti H3K9ac (1:1000; C5B11, Cell signaling) or H3K4me3 (1:1000; C42D8, Cell Signaling Technologies) followed by Alexa fluor 488 goat anti rabbit IgG(H+L) (1:400; A11011, Invitrogen). Cells were counterstained with DAPI.

Proteomics

Three replicates of HeLa-S3 cells (either unsynchronized or STC synchronized) were harvested. Exactly 2.1 million cells from each sample were snap-frozen in liquid nitrogen and stored at -80^0C. Cell pellets were processed for histone modification proteomics analyses as described previously (Creech et al. 2015).

Chromatin immunoprecipitation followed by sequencing (ChIP-seq)

ChIP-seq was performed either manually on individual samples or automatically using the Bravo liquid handling platform (Agilent model 16050-102, "Bravo") as described previously (Busby et al. 2016). In accordance with our efforts to promote reproducibility, all antibodies used were monoclonal. The following antibodies were used: anti RNA polymerase II 8WG16 (ab817, Abcam), anti H3K4me1 (D1A9, Cell Signaling Technologies), anti H3K4me3 (C42D8, Cell Signaling Technologies), anti H3K9ac (C5B11, Cell Signaling Technologies), anti H3K27ac (D5E4, Cell Signaling Technologies), anti H3K27me3 (C36B11, Cell Signaling Technologies), anti H3K36me3 (D5A7, Cell Signaling Technologies) and anti CTCF G.758.4 (MA5-11187,

Invitrogen).

Bioinformatic analysis

ChIP-Seq reads were aligned to the human genome (hg19) using either BWA (Li and Durbin 2009) or Bowtie (Langmead and Salzberg 2012). Duplicate alignments were removed with Picard Tools MarkDuplicates (http://broadinstitute.github.io/picard/). Only QC-passed reads were used for the analyses. Peak detection on merged replicates (with a whole cell extract dataset as a control) was done using HOMER (Heinz et al. 2010) using default histone style parameters for all histone modifications, and default factor style parameters for PolII and CTCF (CTCF ChIP-seq data was used for defining insulators).

Scatter plots were made from read counts (using bedtools multicov (Quinlan and Hall 2010)) at merged interphase and mitosis peaks and normalized to 10 million total reads. ChromHMM (Chromatin State Discovery and Characterization) genomic annotations were downloaded from the UCSC genome-browser for HeLa-S3 cells (Ernst and Kellis 2013) and combined into five main categories. The ChromHMM distribution plot (**Figure 3C**) shows the percentage of reads in peak regions per ChromHMM annotation.

IGV snapshots show TDF files created from the aligned sequence data (using the count command from IGV tools (Robinson et al. 2011; Thorvaldsdottir et al. 2013)). The scale of each track was adjusted to the total number of reads using the Normalize Coverage Data option in IGV, that multiplies each value by [1,000,000 / (totalReadCount)] (**Figures 1C** and **3A**).

For generating coverage profiles, metagene plots, and delta plots, we first fixed the length of each read to the average of the mitosis and interphase fragment length modes. We analyzed the following NDRs – TSS (using gene coordinates from UCSC (Karolchik et al. 2004)), Enhancers (using regions with H3K4me1, H3K27ac, and UCSC P300 HeLa-S3 peak regions (wgEncodeEH001820)), and insulators (using merged interphase and mitosis CTCF ChIP-seq peaks), each containing a unique set of loci. Only regions located >6Kb from each other, and overlapping modification peaks within 500bp on either side of the NDR, were included in the analysis.

Coverage profiles (heat maps) were created from the read depth (calculated using samtools bedcov (Li et al. 2009)) of each modification in a window of 6kb around the NDR in 25bp bins. Read depth was normalized to 10 million total reads, and the depths of each row were then standardized to the range [0,1]. Heat maps are sorted by NDR occupancy in interphase.

Combined coverage profiles (**Figures 5A and S9**) only include regions with peaks for all of the modifications of interest overlapping the NDR. The normalized read depth was converted to a z-score for mitosis and interphase of each modification separately, and then each row was standardized (to [0,1]). Heat maps are sorted by TSS occupancy of H3K9ac in mitosis. Visual inspection of the sorted profiles revealed gene groups based on the combination of modifications at the TSS. Metagene plots were produced by averaging the coverage profiles. Delta plots were made by averaging the result of subtracting the interphase coverage profiles from the mitosis coverage profiles.

For the boxplots (**Figure 5C**), GC content was measured around the TSS (+/-500bp) of genes using bedtools nuc, and corresponding p-values (t-test) and effect sizes were calculated.

HDAC2 and HDAC6 peaks for CD4 (Wang et al. 2009) and K562 cells (Ram et al. 2011) were downloaded and merged. The percentage of genes in each group that overlapped an HDAC peak at the TSS (one bp) was determined and p-values were calculated using a chi-squared test.

ChIP-seq datasets were downloaded from ENCODE (see **Table S1** for ENCODE file names) and metagene profiles of gene groups were created using deepTools plotProfile (Ramirez et al. 2016). Counts at the TSS (20bp on either side) were totaled and corresponding p-values (t-test) were calculated.

Figure legends

Figure 1. Efficient metaphase synchronization of HeLa-S3cells using a kinesin 5 inhibitor (STC) reveals low levels of RNA PolII binding during metaphase. (A) Schematic representation of the synchronization approach. **(B)** Synchronization was monitored by microscopy using both DAPI (blue) and Lamin B (red) staining. Only cells with the monopolar spindle appearance of the chromosomes and lack of nuclear envelope were counted as metaphase stage. The percentage of cells in interphase (blue) and metaphase (red) are shown for both conditions, along with the standard error (SE). For simplicity, we refer to the unsynchronized population as "interphase" and to the synchronized one as "mitosis". **(C)** Integrative genomic viewer (IGV)(Robinson et al. 2011; Thorvaldsdottir et al. 2013) tracks showing the alignment for RNA PolII ChIP-seq results on an approximately 180Kb region on chromosome 1. The image demonstrates reduced levels of RNA PolII binding in metaphase sample (red) compared to interphase sample (blue). When compared to a simulation data resembling the amount of interphase cells in the mitotic sample (10% of interphase reads were mixed with 90% WCE reads), demonstrates the signal in mitotic samples includes binding within mitotic cells. Control sample (whole cell extract, black) is added at the bottom. **(D)** Scatter plots showing the coverage of RNA PolII peaks in mitosis versus interphase after normalization to $1x10^7$ reads and in the simulated sample (shown in **C**) versus mitosis.

Figure 2. Identification of global changes in histone H3 modifications by quantitative targeted mass spectrometry analysis. (A) Heatmap (Log2 of fold change) of the different histone modifications as detailed on top. The major histone modifications are highlighted at the bottom. Data was normalized to average signal of interphase samples. **(B)** Relative abundance of selected modifications on H3 tails from interphase or mitotic HeLa-S3 cells. The data was obtained by quantitative targeted mass spectrometry analysis. Each bar represents the percentage of the H3 peptides with the indicated modifications within the total H3 tail peptide population. Note the high levels of the mitosis unique modification, H3S10ph (~17 fold increase, p-value$<10^{-3}$; two side t-test), providing evidence supporting the tight synchronization of the mitotic samples. Similar results were obtained for H4 modifications (**Figure S2**)

Figure 3. High concordance between mitotic and interphase histone modification patterns. (A) Integrative genomic viewer (IGV) (Robinson et al. 2011; Thorvaldsdottir et al. 2013) tracks showing the alignment for the indicated histone modification ChIP-seq results for interphase (blue) and mitosis (red) samples on an approximately 315Kb region on chromosome 12. The

scale of each track was adjusted to the total number of reads using the Normalize Coverage Data option in IGV (see methods). The ChromHMM annotation for each genomic region is shown below the plot using the same color code as in **C**. **(B)** Scatter plots showing the normalized reads counts for all regions enriched in each modification (see methods for the peak calling details) in mitosis versus interphase. **(C)** Bar plots showing the percentage of reads in peak regions per five ChromHMM categories.

Figure 4. The nucleosomes that enter the NDRs during mitosis are distinguishable from the surrounding nucleosomes. Top: heat maps showing the normalized and standardized read depth at 6Kb centered at either TSS, enhancers, or insulators, for H3K4 methylations (n=6488, 7062, 4367; respectively. (**A**)), and H3K9 or H3K27 acetylations (n=6808, 5565, 3033; respectively. (**B**)). Bottom: "Metagene plots" showing the average read depth for all regions in each category are under the relevant heat map.

Figure 5. Characterization of the TSS associated NDRs. (A) A heat map showing the normalized and standardized z-scores at 6Kb regions centered at TSS of 5731 genes that are occupied by H3K4me3, H3K9ac, and H3K27ac. The regions were manually divided into four groups after visual inspection and the percentage of regions in each group is shown in parentheses. **(B)** Metagene plots showing the average occupancy of each modification for the four groups. **(C)** Boxplot showing the difference in the GC content at the TSS for groups 1-3. The difference between group 1 and both 2 and 3 is highly significant (p-value = 1.67e-133 and 3.97e-84; t-test, and effect size = 0.88 and 1.12, respectively). **(D)** Metagene plots showing ENCODE ChIP-seq data for groups 1-3, p-values were obtained either by comparing group 1 to the combination of groups 2 and 3 (for HCFC1, Brca1, NfyB, and MXI1), or by determining the maximal p-value from all pairwise comparisons (for HA-E2F1 and USF1). For a comprehensive list of all p-values see **Table S1**. The same analysis for all available ENCODE data in HeLa-S3 is shown in **Figures S11-S12**.

Figure 6. Nucleosome shifting and de-acetylation may explain NDR disappearance. (A) Delta metagene plots (see methods for details) showing the average read depth of the indicated modifications after subtracting the interphase depths from the mitotic ones. **(B)** A Scatter plot showing the normalized read counts at peaks for H3K9ac ChIP-seq on cells treated with TSA in mitosis versus interphase. **(C)** Metagene and **(D)** Delta metagene plots for ChIP-seq data after TSA treatment. Similar results were obtained in a biological replicate (**Figure S13**).

Acknowledgments

We thank Dr. Michelle Busby and Dr. Melisa Gymrek for fruitful discussions, Yutong Qiu, Miguel Alcantar and Michal Schlesinger for technical assistance, and Jason Ernst for assistance with HeLa-S3 ChromHMM data. This research was supported by the Israel Science Foundation (grant no. 184/16 to IS), the Israel Science Foundation – Broad Institute Joint Program (grant no. 1972/15 to IS and AG), the United States-Israel Binational Science Foundation (BSF), Jerusalem, Israel (grant no. 2015272 to IS and AG), and NIH grant (U54 HG008097 to JDJ).

Data accessibility

Pending submission to SRA.

References

Antonin W, Neumann H. 2016. Chromosome condensation and decondensation during mitosis. *Curr Opin Cell Biol* **40**: 15-22.

Bailey TL. 2011. DREME: motif discovery in transcription factor ChIP-seq data. *Bioinformatics* **27**: 1653-1659.

Bar-Joseph Z, Siegfried Z, Brandeis M, Brors B, Lu Y, Eils R, Dynlacht BD, Simon I. 2008. Genome-wide transcriptional analysis of the human cell cycle identifies genes differentially regulated in normal and cancer cells. *Proceedings of the National Academy of Sciences of the United States of America* **105**: 955-960.

Belmont AS, Bruce K. 1994. Visualization of G1 chromosomes: a folded, twisted, supercoiled chromonema model of interphase chromatid structure. *J Cell Biol* **127**: 287-302.

Black LK, Petruk S, Fenstermaker TK, Hodgson JW, Caplan JL, Brock HW, Mazo A. 2016. Chromatin proteins and RNA are associated with DNA during all phases of mitosis. *Cell Discov* **2**: 16038.

Busby M, Xue C, Li C, Farjoun Y, Gienger E, Yofe I, Gladden A, Epstein CB, Cornett EM, Rothbart SB et al. 2016. Systematic comparison of monoclonal versus polyclonal antibodies for mapping histone modifications by ChIP-seq. *Epigenetics Chromatin* **9**: 49.

Caravaca JM, Donahue G, Becker JS, He X, Vinson C, Zaret KS. 2013. Bookmarking by specific and nonspecific binding of FoxA1 pioneer factor to mitotic chromosomes. *Genes & development* **27**: 251-260.

Chen D, Dundr M, Wang C, Leung A, Lamond A, Misteli T, Huang S. 2005. Condensed mitotic chromatin is accessible to transcription factors and chromatin structural proteins. *J Cell Biol* **168**: 41-54.

Cho RJ, Huang M, Campbell MJ, Dong H, Steinmetz L, Sapinoso L, Hampton G, Elledge SJ, Davis RW, Lockhart DJ. 2001. Transcriptional regulation and function during the human cell cycle. *Nature genetics* **27**: 48-54.

Cimini D, Mattiuzzo M, Torosantucci L, Degrassi F. 2003. Histone hyperacetylation in mitosis prevents sister chromatid separation and produces chromosome segregation defects. *Mol Biol Cell* **14**: 3821-3833.

Creech AL, Taylor JE, Maier VK, Wu X, Feeney CM, Udeshi ND, Peach SE, Boehm JS, Lee JT, Carr SA et al. 2015. Building the Connectivity Map of epigenetics: chromatin profiling by quantitative targeted mass spectrometry. *Methods* **72**: 57-64.

Dileep V, Ay F, Sima J, Vera DL, Noble WS, Gilbert DM. 2015. Topologically associating domains and their long-range contacts are established during early G1 coincident with the establishment of the replication-timing program. *Genome research* **25**: 1104-1113.

Ernst J, Kellis M. 2012. ChromHMM: automating chromatin-state discovery and characterization. *Nat Methods* **9**: 215-216.

Ernst J, Kellis M. 2013. Interplay between chromatin state, regulator binding, and regulatory motifs in six human cell types. *Genome research* **23**: 1142-1154.

Gazit B, Cedar H, Lerer I, Voss R. 1982. Active genes are sensitive to deoxyribonuclease I during metaphase. *Science* **217**: 648-650.

Gottesfeld JM, Forbes DJ. 1997. Mitotic repression of the transcriptional machinery. *Trends Biochem Sci* **22**: 197-202.

Halley-Stott RP, Jullien J, Pasque V, Gurdon J. 2014. Mitosis gives a brief window of opportunity for a change in gene transcription. *PLoS Biol* **12**: e1001914.

Heinz S, Benner C, Spann N, Bertolino E, Lin YC, Laslo P, Cheng JX, Murre C, Singh H, Glass CK. 2010. Simple combinations of lineage-determining transcription factors prime cis-regulatory elements required for macrophage and B cell identities. *Molecular cell* **38**: 576-589.

Hendzel MJ, Wei Y, Mancini MA, Van Hooser A, Ranalli T, Brinkley BR, Bazett-Jones DP, Allis CD. 1997. Mitosis-specific phosphorylation of histone H3 initiates primarily within pericentromeric heterochromatin during G2 and spreads in an ordered fashion coincident with mitotic chromosome condensation. *Chromosoma* **106**: 348-360.

Henikoff S. 2008. Nucleosome destabilization in the epigenetic regulation of gene expression. *Nat Rev Genet* **9**: 15-26.

Hsiung CC, Bartman CR, Huang P, Ginart P, Stonestrom AJ, Keller CA, Face C, Jahn KS, Evans P, Sankaranarayanan L et al. 2016. A hyperactive transcriptional state marks genome reactivation at the mitosis-G1 transition. *Genes & development* **30**: 1423-1439.

Hsiung CC, Morrissey CS, Udugama M, Frank CL, Keller CA, Baek S, Giardine B, Crawford GE, Sung MH, Hardison RC et al. 2015. Genome accessibility is widely preserved and locally modulated during mitosis. *Genome research* **25**: 213-225.

Jaffe JD, Wang Y, Chan HM, Zhang J, Huether R, Kryukov GV, Bhang HE, Taylor JE, Hu M, Englund NP et al. 2013. Global chromatin profiling reveals NSD2 mutations in pediatric acute lymphoblastic leukemia. *Nature genetics* **45**: 1386-1391.

Jin C, Felsenfeld G. 2007. Nucleosome stability mediated by histone variants H3.3 and H2A.Z. *Genes Dev* **21**: 1519-1529.

Johansen KM, Johansen J. 2006. Regulation of chromatin structure by histone H3S10 phosphorylation. *Chromosome research : an international journal on the molecular, supramolecular and evolutionary aspects of chromosome biology* **14**: 393-404.

Kadauke S, Blobel GA. 2013. Mitotic bookmarking by transcription factors. *Epigenetics & chromatin* **6**: 6.

Kadauke S, Udugama MI, Pawlicki JM, Achtman JC, Jain DP, Cheng Y, Hardison RC, Blobel GA. 2012. Tissue-specific mitotic bookmarking by hematopoietic transcription factor GATA1. *Cell* **150**: 725-737.

Karolchik D, Hinrichs AS, Furey TS, Roskin KM, Sugnet CW, Haussler D, Kent WJ. 2004. The UCSC Table Browser data retrieval tool. *Nucleic acids research* **32**: D493-496.

Kelly TK, Miranda TB, Liang G, Berman BP, Lin JC, Tanay A, Jones PA. 2010. H2A.Z maintenance during mitosis reveals nucleosome shifting on mitotically silenced genes. *Mol Cell* **39**: 901-911.

King DW, Barnhisel ML. 1967. Synthesis of RNA in mammalian cells during mitosis and interphase. *J Cell Biol* **33**: 265-272.

Kouskouti A, Talianidis I. 2005. Histone modifications defining active genes persist after transcriptional and mitotic inactivation. *EMBO J* **24**: 347-357.

Langmead B, Salzberg SL. 2012. Fast gapped-read alignment with Bowtie 2. *Nature methods* **9**: 357-359.

Lee CK, Shibata Y, Rao B, Strahl BD, Lieb JD. 2004. Evidence for nucleosome depletion at active regulatory regions genome-wide. *Nature genetics* **36**: 900-905.

Li H, Durbin R. 2009. Fast and accurate short read alignment with Burrows-Wheeler transform. *Bioinformatics* **25**: 1754-1760.

Li H, Handsaker B, Wysoker A, Fennell T, Ruan J, Homer N, Marth G, Abecasis G, Durbin R, Genome Project Data Processing S. 2009. The Sequence Alignment/Map format and SAMtools. *Bioinformatics* **25**: 2078-2079.

Li M, Sun Q, Wang X. 2017. Transcriptional landscape of human cancers. *Oncotarget* **8**: 34534-34551.

Li Y, Kao GD, Garcia BA, Shabanowitz J, Hunt DF, Qin J, Phelan C, Lazar MA. 2006. A novel histone deacetylase pathway regulates mitosis by modulating Aurora B kinase activity. *Genes Dev* **20**: 2566-2579.

Liang K, Woodfin AR, Slaughter BD, Unruh JR, Box AC, Rickels RA, Gao X, Haug JS, Jaspersen SL, Shilatifard A. 2015. Mitotic Transcriptional Activation: Clearance of Actively Engaged Pol II via Transcriptional Elongation Control in Mitosis. *Mol Cell* **60**:

435-445.
Liu Y, Chen S, Wang S, Soares F, Fischer M, Meng F, Du Z, Lin C, Meyer C, DeCaprio JA et al. 2017a. Transcriptional landscape of the human cell cycle. *Proc Natl Acad Sci U S A* **114**: 3473-3478.
Liu Y, Pelham-Webb B, Di Giammartino DC, Li J, Kim D, Kita K, Saiz N, Garg V, Doane A, Giannakakou P et al. 2017b. Widespread Mitotic Bookmarking by Histone Marks and Transcription Factors in Pluripotent Stem Cells. *Cell Rep* **19**: 1283-1293.
Long HK, Prescott SL, Wysocka J. 2016. Ever-Changing Landscapes: Transcriptional Enhancers in Development and Evolution. *Cell* **167**: 1170-1187.
Martinez-Balbas MA, Dey A, Rabindran SK, Ozato K, Wu C. 1995. Displacement of sequence-specific transcription factors from mitotic chromatin. *Cell* **83**: 29-38.
Matsui Y, Nakayama Y, Okamoto M, Fukumoto Y, Yamaguchi N. 2012. Enrichment of cell populations in metaphase, anaphase, and telophase by synchronization using nocodazole and blebbistatin: a novel method suitable for examining dynamic changes in proteins during mitotic progression. *Eur J Cell Biol* **91**: 413-419.
Nagai S, Davis RE, Mattei PJ, Eagen KP, Kornberg RD. 2017. Chromatin potentiates transcription. *Proc Natl Acad Sci U S A* **114**: 1536-1541.
Naumova N, Imakaev M, Fudenberg G, Zhan Y, Lajoie BR, Mirny LA, Dekker J. 2013. Organization of the mitotic chromosome. *Science* **342**: 948-953.
Noh EJ, Lim DS, Jeong G, Lee JS. 2009. An HDAC inhibitor, trichostatin A, induces a delay at G2/M transition, slippage of spindle checkpoint, and cell death in a transcription-dependent manner. *Biochem Biophys Res Commun* **378**: 326-331.
Palozola KC, Donahue G, Liu H, Grant GR, Becker JS, Cote A, Yu H, Raj A, Zaret KS. 2017. Mitotic transcription and waves of gene reactivation during mitotic exit. *Science* doi:10.1126/science.aal4671.
Parsons GG, Spencer CA. 1997. Mitotic repression of RNA polymerase II transcription is accompanied by release of transcription elongation complexes. *Mol Cell Biol* **17**: 5791-5802.
Prasanth KV, Sacco-Bubulya PA, Prasanth SG, Spector DL. 2003. Sequential entry of components of the gene expression machinery into daughter nuclei. *Mol Biol Cell* **14**: 1043-1057.
Prescott DM, Bender MA. 1962. Synthesis of RNA and protein during mitosis in mammalian tissue culture cells. *Exp Cell Res* **26**: 260-268.
Quinlan AR, Hall IM. 2010. BEDTools: a flexible suite of utilities for comparing genomic features. *Bioinformatics* **26**: 841-842.
Ram O, Goren A, Amit I, Shoresh N, Yosef N, Ernst J, Kellis M, Gymrek M, Issner R, Coyne M et al. 2011. Combinatorial patterning of chromatin regulators uncovered by genome-wide location analysis in human cells. *Cell* **147**: 1628-1639.
Ramirez F, Ryan DP, Gruning B, Bhardwaj V, Kilpert F, Richter AS, Heyne S, Dundar F, Manke T. 2016. deepTools2: a next generation web server for deep-sequencing data analysis. *Nucleic acids research* **44**: W160-165.
Raynaud C, Mallory AC, Latrasse D, Jegu T, Bruggeman Q, Delarue M, Bergounioux C, Benhamed M. 2014. Chromatin meets the cell cycle. *J Exp Bot* **65**: 2677-2689.
Robinson JT, Thorvaldsdottir H, Winckler W, Guttman M, Lander ES, Getz G, Mesirov JP. 2011. Integrative genomics viewer. *Nature biotechnology* **29**: 24-26.
Skoufias DA, DeBonis S, Saoudi Y, Lebeau L, Crevel I, Cross R, Wade RH, Hackney D, Kozielski F. 2006. S-trityl-L-cysteine is a reversible, tight binding inhibitor of the human kinesin Eg5 that specifically blocks mitotic progression. *J Biol Chem* **281**: 17559-17569.
Spellman PT, Sherlock G, Zhang MQ, Iyer VR, Anders K, Eisen MB, Brown PO, Botstein D, Futcher B. 1998. Comprehensive identification of cell cycle-regulated genes of the yeast Saccharomyces cerevisiae by microarray hybridization. *Mol Biol Cell* **9**: 3273-3297.

Stevens TJ, Lando D, Basu S, Atkinson LP, Cao Y, Lee SF, Leeb M, Wohlfahrt KJ, Boucher W, O'Shaughnessy-Kirwan A et al. 2017. 3D structures of individual mammalian genomes studied by single-cell Hi-C. *Nature* **544**: 59-64.

Struhl K, Segal E. 2013. Determinants of nucleosome positioning. *Nat Struct Mol Biol* **20**: 267-273.

Swygert SG, Peterson CL. 2014. Chromatin dynamics: interplay between remodeling enzymes and histone modifications. *Biochimica et biophysica acta* **1839**: 728-736.

Taylor JH. 1960. Nucleic acid synthesis in relation to the cell division cycle. *Ann N Y Acad Sci* **90**: 409-421.

Teves SS, An L, Hansen AS, Xie L, Darzacq X, Tjian R. 2016. A dynamic mode of mitotic bookmarking by transcription factors. *Elife* **5**.

Thorvaldsdottir H, Robinson JT, Mesirov JP. 2013. Integrative Genomics Viewer (IGV): high-performance genomics data visualization and exploration. *Brief Bioinform* **14**: 178-192.

Tsompana M, Buck MJ. 2014. Chromatin accessibility: a window into the genome. *Epigenetics Chromatin* **7**: 33.

Vagnarelli P. 2013. Chromatin reorganization through mitosis. *Adv Protein Chem Struct Biol* **90**: 179-224.

Valls E, Sanchez-Molina S, Martinez-Balbas MA. 2005. Role of histone modifications in marking and activating genes through mitosis. *J Biol Chem* **280**: 42592-42600.

Van Hooser A, Goodrich DW, Allis CD, Brinkley BR, Mancini MA. 1998. Histone H3 phosphorylation is required for the initiation, but not maintenance, of mammalian chromosome condensation. *J Cell Sci* **111 (Pt 23)**: 3497-3506.

Wang F, Higgins JM. 2013. Histone modifications and mitosis: countermarks, landmarks, and bookmarks. *Trends in cell biology* **23**: 175-184.

Wang Z, Zang C, Cui K, Schones DE, Barski A, Peng W, Zhao K. 2009. Genome-wide mapping of HATs and HDACs reveals distinct functions in active and inactive genes. *Cell* **138**: 1019-1031.

Whitfield ML, Sherlock G, Saldanha AJ, Murray JI, Ball CA, Alexander KE, Matese JC, Perou CM, Hurt MM, Brown PO et al. 2002. Identification of genes periodically expressed in the human cell cycle and their expression in tumors. *Mol Biol Cell* **13**: 1977-2000.

Zaidi SK, Grandy RA, Lopez-Camacho C, Montecino M, van Wijnen AJ, Lian JB, Stein JL, Stein GS. 2014. Bookmarking target genes in mitosis: a shared epigenetic trait of phenotypic transcription factors and oncogenes? *Cancer Res* **74**: 420-425.

Zhao R, Nakamura T, Fu Y, Lazar Z, Spector DL. 2011. Gene bookmarking accelerates the kinetics of post-mitotic transcriptional re-activation. *Nature cell biology* **13**: 1295-1304.

Zhou VW, Goren A, Bernstein BE. 2011. Charting histone modifications and the functional organization of mammalian genomes. *Nat Rev Genet* **12**: 7-18.

Figure 1

A

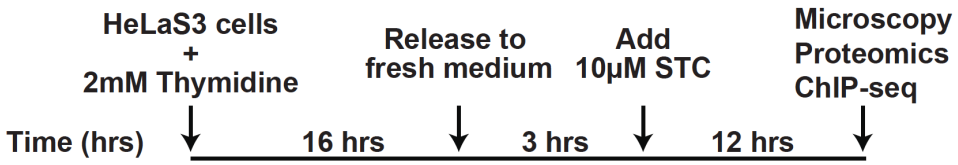

B

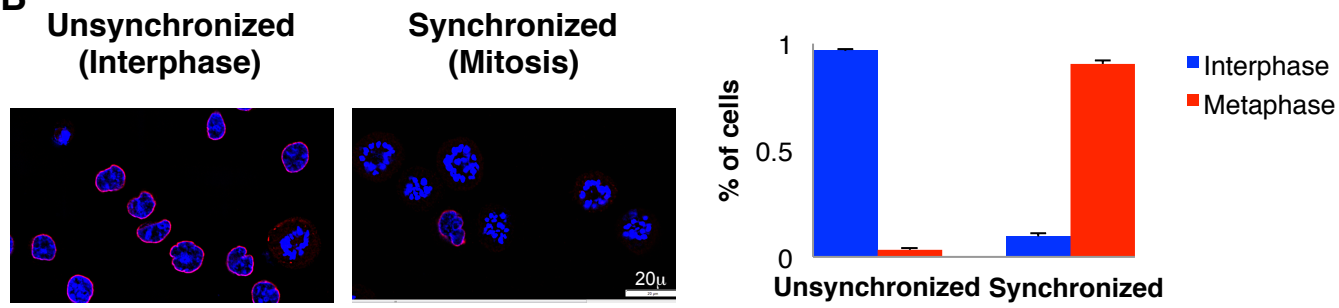

C

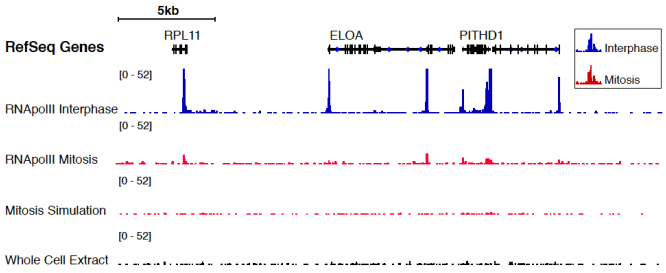

D

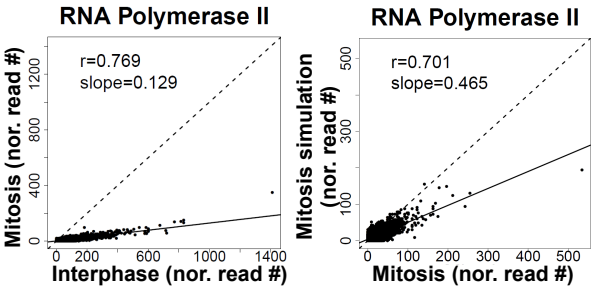

Figure 2

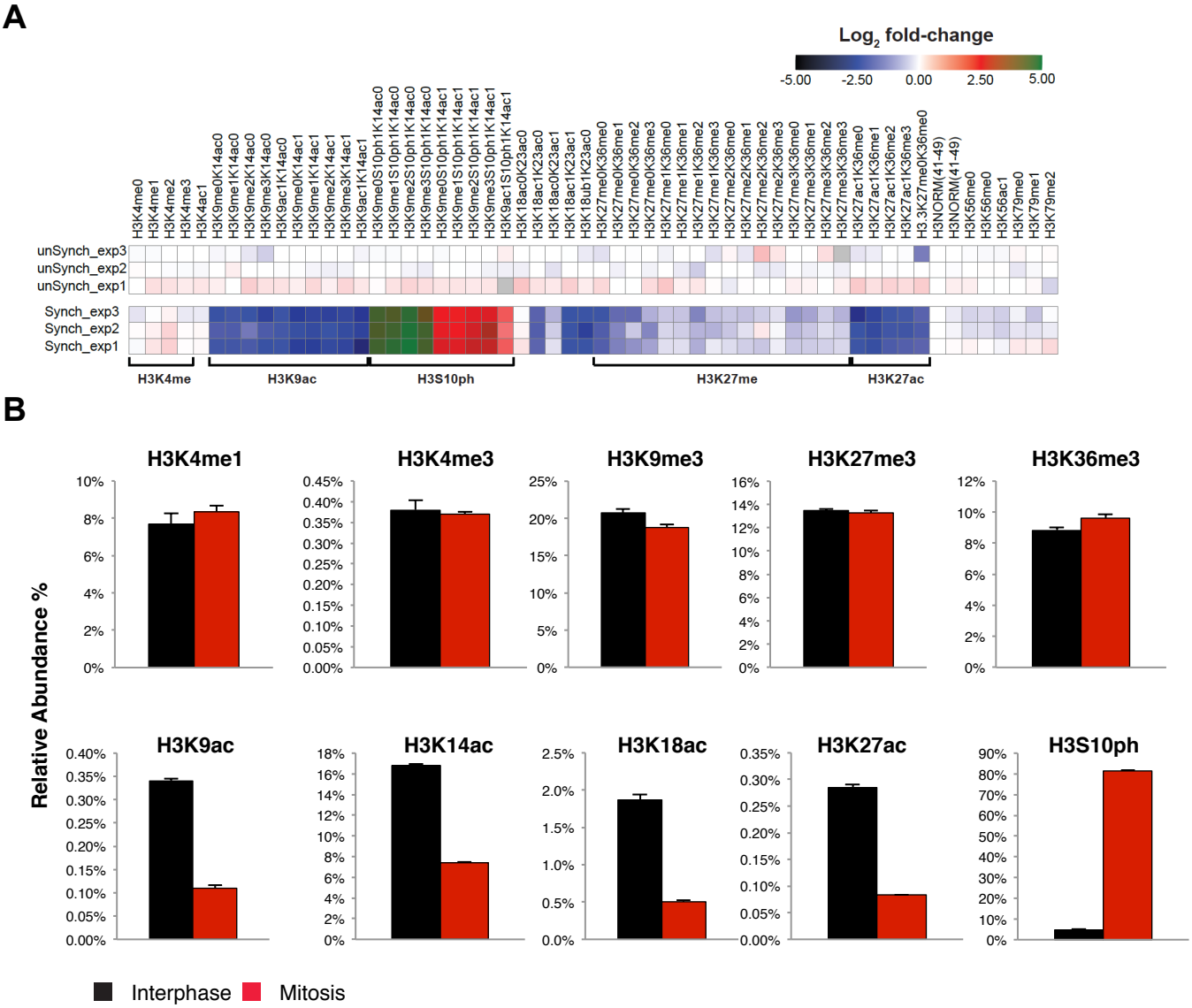
A
Log2 fold-change
-5.00
-2.50
0.00
2.50
5.00
H3K4me0
H3K4me1
H3K4me2
H3K4me3
H3K4ac1
H3K9me0K14ac0
H3K9me1K14ac0
H3K9me2K14ac0
H3K9me3K14ac0
H3K9ac1K14ac0
H3K9me0K14ac1
H3K9me1K14ac1
H3K9me2K14ac1
H3K9me3K14ac1
H3K9ac1K14ac1
H3K9me0S10ph1K14ac0
H3K9me1S10ph1K14ac0
H3K9me2S10ph1K14ac0
H3K9me3S10ph1K14ac0
H3K9me0S10ph1K14ac1
H3K9me1S10ph1K14ac1
H3K9me2S10ph1K14ac1
H3K9me3S10ph1K14ac1
H3K9ac1S10ph1K14ac1
H3K18ac0K23ac0
H3K18ac1K23ac0
H3K18ac0K23ac1
H3K18ac1K23ac1
H3K18ub1K23ac0
H3K27me0K36me0
H3K27me0K36me1
H3K27me0K36me2
H3K27me0K36me3
H3K27me1K36me0
H3K27me1K36me1
H3K27me1K36me2
H3K27me1K36me3
H3K27me2K36me0
H3K27me2K36me1
H3K27me2K36me2
H3K27me2K36me3
H3K27me3K36me0
H3K27me3K36me1
H3K27me3K36me2
H3K27me3K36me3
H3K27ac1K36me0
H3K27ac1K36me1
H3K27ac1K36me2
H3K27ac1K36me3
H3.3K27me0K36me0
H3NORM(41-49)
H3NORM(41-49)
H3K56me0
H3K56me0
H3K56ac1
H3K79me0
H3K79me1
H3K79me2
unSynch_exp3
unSynch_exp2
unSynch_exp1
Synch_exp3
Synch_exp2
Synch_exp1
H3K4me
H3K9ac
H3S10ph
H3K27me
H3K27ac
B
Relative Abundance %
H3K4me1
H3K4me3
H3K9me3
H3K27me3
H3K36me3
H3K9ac
H3K14ac
H3K18ac
H3K27ac
H3S10ph
Interphase
Mitosis

Figure 3

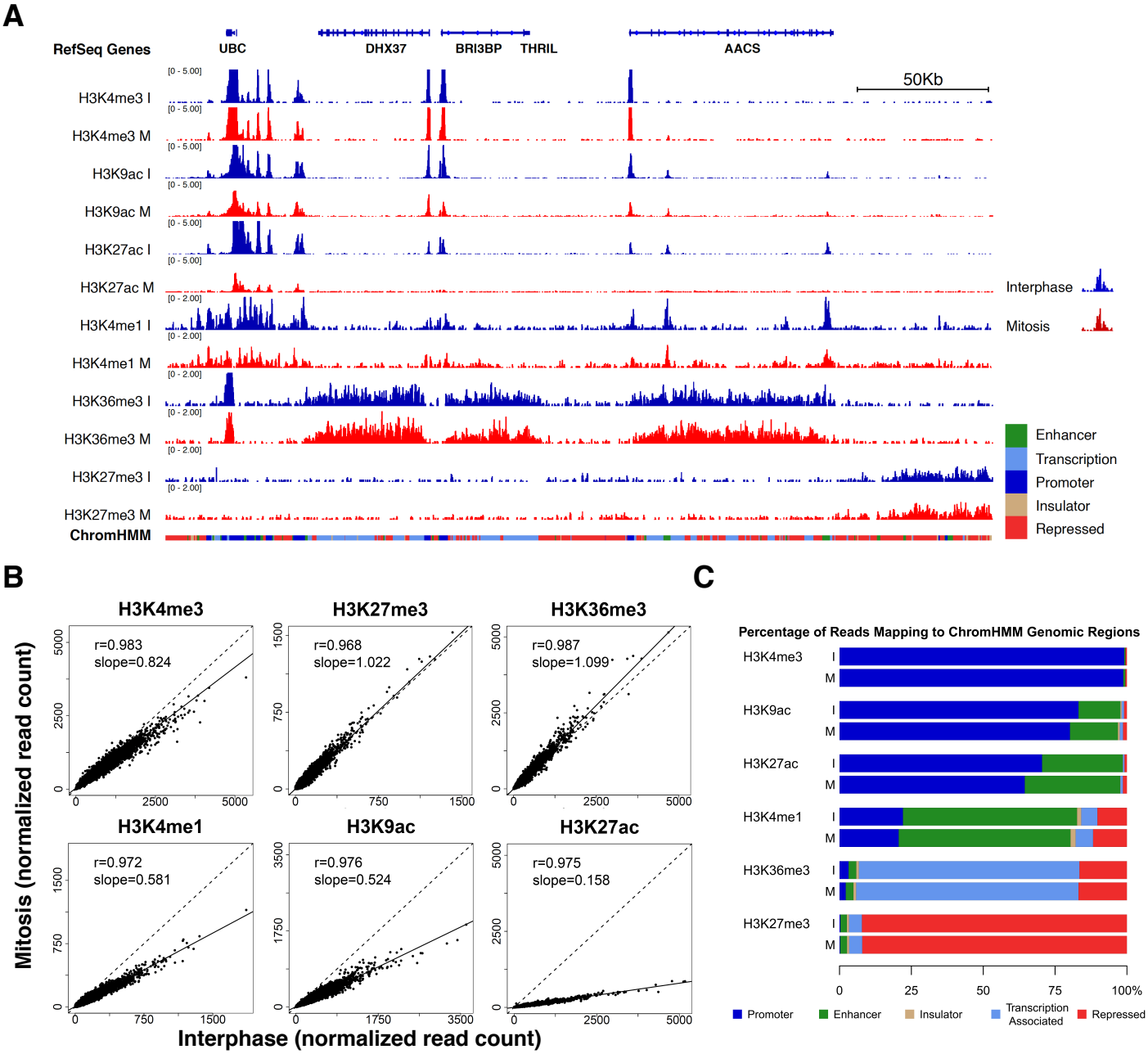
A
RefSeq Genes
UBC
DHX37
BRI3BP
THRIL
AACS
50Kb
H3K4me3 I
H3K4me3 M
H3K9ac I
H3K9ac M
H3K27ac I
H3K27ac M
H3K4me1 I
H3K4me1 M
H3K36me3 I
H3K36me3 M
H3K27me3 I
H3K27me3 M
ChromHMM
Interphase
Mitosis
Enhancer
Transcription
Promoter
Insulator
Repressed
B
H3K4me3
r=0.983
slope=0.824
H3K27me3
r=0.968
slope=1.022
H3K36me3
r=0.987
slope=1.099
H3K4me1
r=0.972
slope=0.581
H3K9ac
r=0.976
slope=0.524
H3K27ac
r=0.975
slope=0.158
Mitosis (normalized read count)
Interphase (normalized read count)
C
Percentage of Reads Mapping to ChromHMM Genomic Regions
H3K4me3
H3K9ac
H3K27ac
H3K4me1
H3K36me3
H3K27me3
I
M
0
25
50
75
100%
Promoter
Enhancer
Insulator
Transcription Associated
Repressed

Figure 4

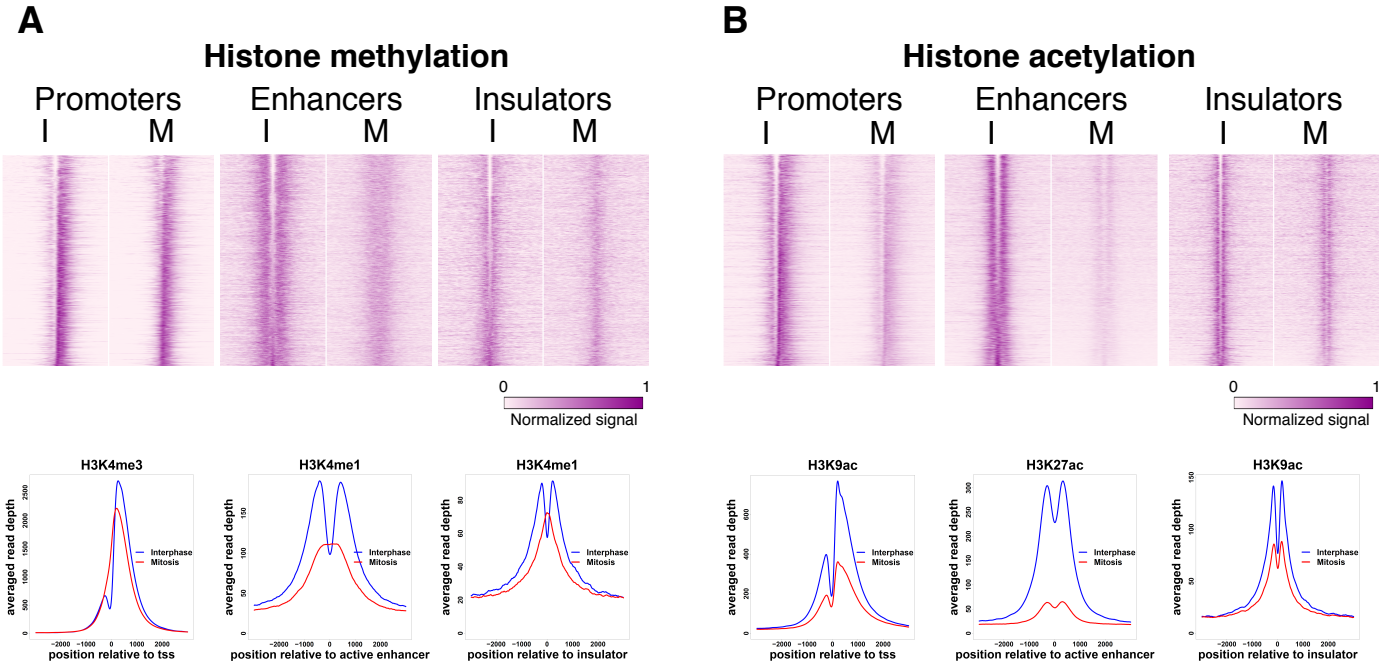
A
Histone methylation
Promoters
Enhancers
Insulators
I
M
0
1
Normalized signal
H3K4me3
H3K4me1
H3K4me1
averaged read depth
Interphase
Mitosis
position relative to tss
position relative to active enhancer
position relative to insulator
B
Histone acetylation
H3K9ac
H3K27ac
H3K9ac

Figure 5

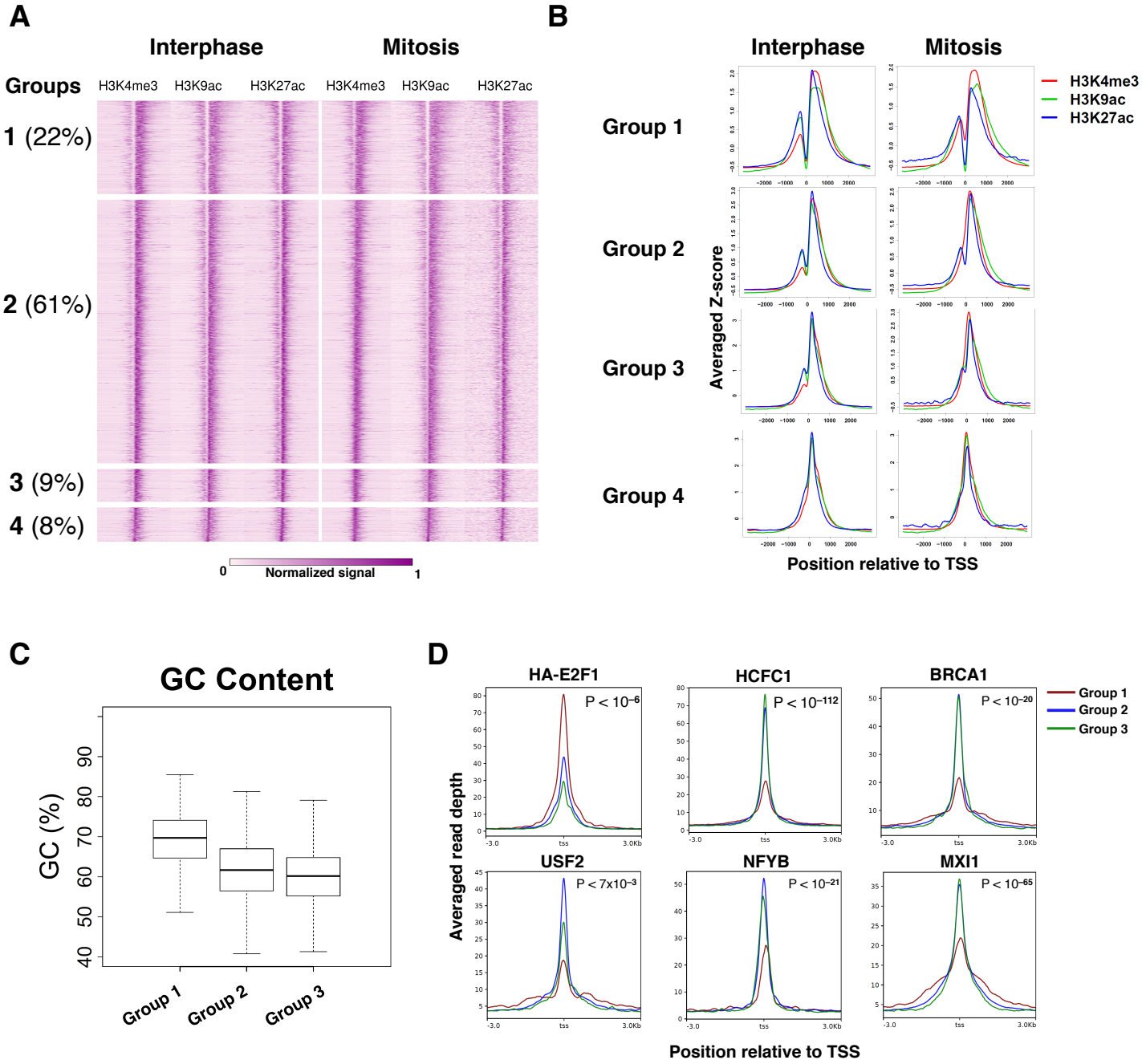
A
Interphase
Mitosis
Groups
H3K4me3
H3K9ac
H3K27ac
H3K4me3
H3K9ac
H3K27ac
1 (22%)
2 (61%)
3 (9%)
4 (8%)
0
Normalized signal
1
B
Interphase
Mitosis
H3K4me3
H3K9ac
H3K27ac
Group 1
Group 2
Group 3
Group 4
Averaged Z-score
Position relative to TSS
C
GC Content
GC (%)
Group 1
Group 2
Group 3
D
HA-E2F1
HCFC1
BRCA1
USF2
NFYB
MXI1
P < 10−6
P < 10−112
P < 10−20
P < 7x10−3
P < 10−21
P < 10−65
Group 1
Group 2
Group 3
Averaged read depth
Position relative to TSS

Figure 6

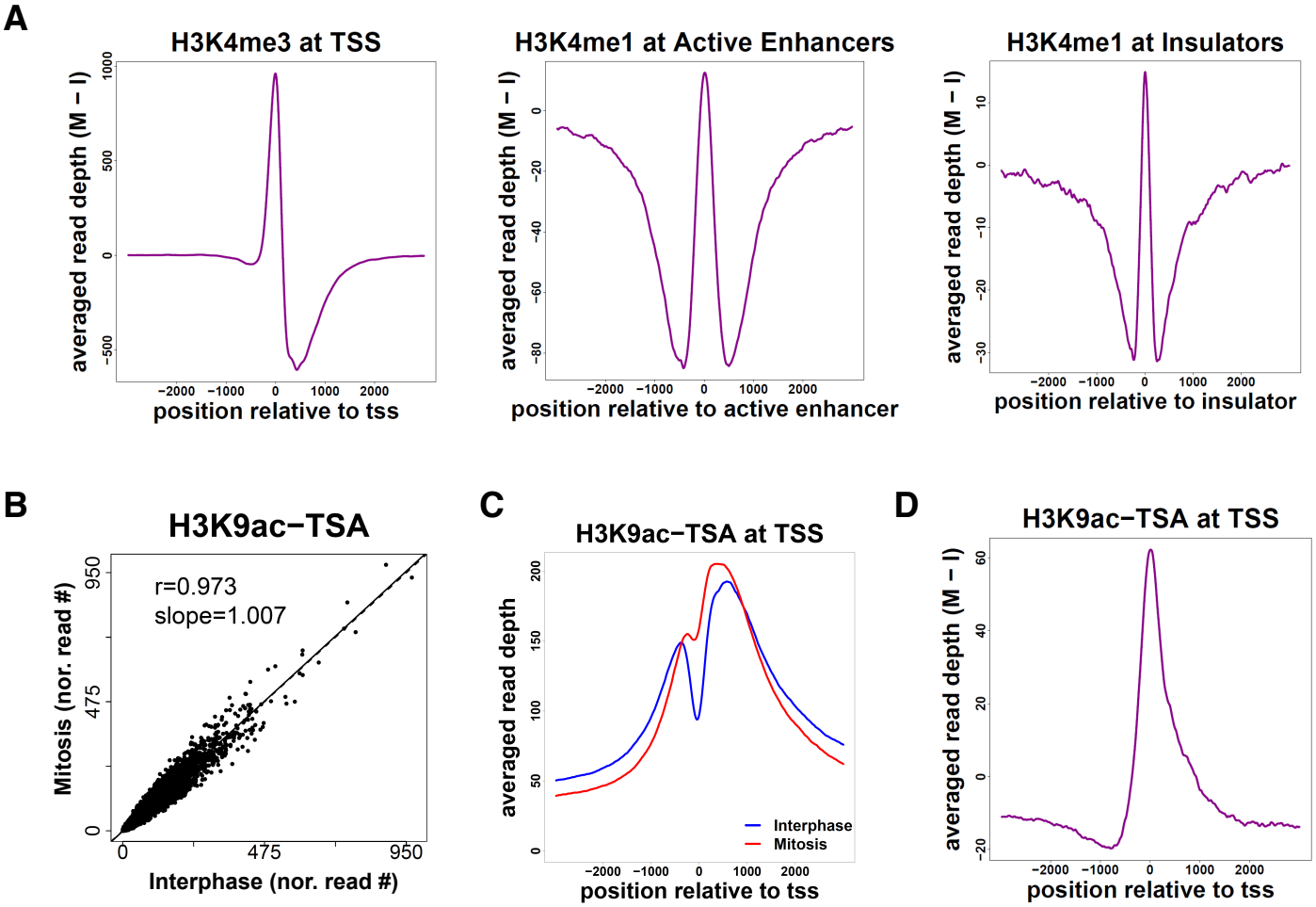
A
H3K4me3 at TSS
averaged read depth (M − I)
position relative to tss
H3K4me1 at Active Enhancers
position relative to active enhancer
H3K4me1 at Insulators
position relative to insulator
B
H3K9ac−TSA
r=0.973
slope=1.007
Mitosis (nor. read #)
Interphase (nor. read #)
C
H3K9ac−TSA at TSS
averaged read depth
Interphase
Mitosis
position relative to tss
D
H3K9ac−TSA at TSS
averaged read depth (M − I)
position relative to tss